Antiviral Research 182 (2020) 104877

Contents lists available at ScienceDirect

Antiviral Research

journal homepage: www.elsevier.com/locate/antiviral

Research paper

Murine norovirus replicase augments RIG-I-like receptors-mediated antiviral interferon response

Peifa Yu, Yang Li, Yunlong Li, Zhijiang Miao, Yining Wang, Maikel P. Peppelenbosch, Qiuwei Pan *

Department of Gastroenterology and Hepatology, Erasmus MC-University Medical Center, Rotterdam, the Netherlands

ARTICLE INFO

Keywords:
Norovirus
NS7
RIG-I
MDA5
ISG

ABSTRACT

Noroviruses are the main causative agents for acute viral gastroenteritis worldwide. RIG-I-like receptors (RLRs) triggered interferon (IFN) activation is essential for host defense against viral infections. In turn, viruses have developed sophisticated strategies to counteract host antiviral response. This study aims to investigate how murine norovirus (MNV) replicase interacts with RLRs-mediated antiviral IFN response. Counterintuitively, we found that the MNV replicase NS7 enhances the activation of poly (I:C)-induced IFN response and the transcription of downstream interferon-stimulated genes (ISGs). Interestingly, NS7 protein augments RIG-I and MDA5-triggered antiviral IFN response, which conceivably involves direct interactions with the caspase activation and recruitment domains (CARDs) of RIG-I and MDA5. Consistently, RIG-I and MDA5 exert anti-MNV activity in human HEK293T cells with ectopic expression of viral receptor CD300lf. This effect requires the activation of JAK/STAT pathway, and is further enhanced by NS7 overexpression. These findings revealed an unconventional role of MNV NS7 as augmenting RLRs-mediated IFN response to inhibit viral replication.

1. Introduction

Human noroviruses (HuNV) are positive sense single-stranded RNA viruses belonging to the *Caliciviridae* family (Karst et al., 2014). Although they are the major causes of epidemic nonbacterial gastroenteritis worldwide (Bok and Green, 2012; Glass et al., 2009), progress on norovirus research has been hampered by the lack of robust cell culture systems. The closely related murine norovirus (MNV) shares similar structural and genetic features with HuNV and can efficiently propagate *in vitro* and *in vivo* (Wobus et al., 2004, 2006). Importantly, the recent discovery of the MNV receptor (CD300lf) breaks the barriers for viral infection in human cells, and enables the study of MNV in human cell models (Orchard et al., 2016, 2019).

The MNV genome is approximately 7.5 kilo bases (kb) in length that encodes four open reading frames (ORFs) (Karst et al., 2014; McFadden et al., 2011). ORF1 encodes a polyprotein that is post-translationally cleaved into six non-structural proteins (NS1/2 to NS7), while ORF2 and ORF3 encode the major and minor structural proteins that referred to as VP1 and VP2, respectively (Zhu et al., 2013). ORF4 overlaps with ORF2, and encodes the virulence factor (VF1), which can antagonize innate immune response to MNV infection (McFadden et al., 2011; Zhu et al., 2013). The non-structural proteins are associated with the viral replication complex induced membrane clusters, and interaction with host factors to regulate cellular homeostasis and promote viral replication (Hyde et al., 2009, 2012). NS7 is the viral RNA-dependent RNA polymerase (RdRp) (Högbom et al., 2009; Zamyatkin et al., 2008), responsible for viral replication.

Interferon (IFN)-mediated innate immune response provides a forward line of cell-autonomous defense against viral infections (Wu and Chen, 2014). Upon infection, viral components can be recognized by specific pathogen recognition receptors including the RIG-I-like receptors (RLRs) RIG-I and MDA5, which subsequently activate IFN response (Kato et al., 2006; Yoneyama et al., 2004). MDA5 has been demonstrated as a predominant sensor of MNV (McCartney et al., 2008), whereas inactivating RIG-I signaling has no effects on HuNV replication (Guix et al., 2007). RIG-I and MDA5 contain the N-terminal caspase-recruitment domains (CARDs), which can recruit and interact with the CARD-containing adaptor named mitochondrial antiviral signaling protein (also known as IPS-1, VISA or Cardif) (Kawai et al., 2005; Seth et al., 2005). The interaction stimulates downstream

* Corresponding author. Department of Gastroenterology and Hepatology, Erasmus MC, room Na-1005, 's-Gravendijkwal 230, NL-3015 CE, Rotterdam, the Netherlands.
E-mail address: q.pan@erasmusmc.nl (Q. Pan).

https://doi.org/10.1016/j.antiviral.2020.104877
Received 22 April 2020; Received in revised form 5 July 2020; Accepted 6 July 2020
Available online 2 August 2020

signaling pathways including activation of transcriptional factors NF-kB and IRF3, and further induces type I IFN production (Honda et al., 2006; Seth et al., 2005). The released IFNs bind to their receptors and in turn activate Janus kinase (JAK)/signal transducer and activator of transcription (STAT) signaling pathway, leading to transcription of hundreds of interferon-stimulated genes (ISGs), some of which are considered as the ultimate antiviral effectors restricting viral replication (Schoggins et al., 2011).

Many viruses have developed sophisticated strategies to counteract the host IFN signaling. For instance, MNV VF1 can inhibit RLRs-mediated IFN response (Zhu et al., 2013), and VP2 has been reported to possess important functions in viral replication and modulation of the host immune response (Zhu et al., 2013). Studies have reported the regulation of viral replicases on RIG-I and MDA5 mediated IFN response. Semliki Forest virus (SFV) RdRp can induce IFN-β through the RIG-I and MDA5 pathways by converting host cell RNA into 5′-ppp RNA (Nikonov et al., 2013). Furthermore, transgenic mice stably expressing RdRp encoded by Theiler's murine encephalomyelitis virus (TMEV) can dramatically upregulate antiviral ISGs and confer profound resistance to ECMV challenge, and is refractory to HIV-1 infection in THP-1 cells (Painter et al., 2015). Recently, transgenic mice with similar antiviral mechanisms against retrovirus infection have also been documented (Miller et al., 2020). Previous studies have revealed that RNAs synthesized by transiently expression of norovirus RdRp can stimulate RIG-I-dependent reporter luciferase production via the IFN-β promoter (Subba-Reddy et al., 2011). However, a recent study showed that the replicases of enterovirus 71 (EV71) and coxsackievirus B3 inhibit MDA5-mediated IFN activation through interaction with MDA5 (Kuo et al., 2019). Given the importance and complicity of interactions between viral replicases with the host innate immunity, this study aims to investigate the role of MNV NS7 on regulating RLRs-mediated IFN activation and antiviral response.

2. Materials and methods

2.1. Reagents

Poly (I:C) (HMW) (Bio-Connect BV) was dissolved in distilled water. Stocks of JAK inhibitor 1 (SC-204021, Santa Cruz Biotechnology, Santa Cruz, CA, USA) were dissolved in DMSO (DMSO, Sigma, Zwijndrecht, the Netherlands) with a final concentration of 5 mg/ml. Halt™ Protease Inhibitor Cocktail (100X) was purchased from Thermo Fisher Scientific. Rabbit polyclonal antisera to MNV NS1/2 was kindly provided by Prof. Vernon K. Ward (School of Biomedical Sciences, University of Otago, New Zealand) (Davies et al., 2015). Rabbit polyclonal antisera to MNV NS7 was kindly provided by Prof. Ian Goodfellow (Department of Pathology, University of Cambridge, UK) (Emmott et al., 2019). Mouse anti-RIG-I (clone 1C3, Sigma) and mouse anti-MDA5 (Proteintech) antibodies were used. β-actin antibody (#sc-47778) was purchased from Santa Cruz Biotechnology. IRDye® 800CW-conjμgated goat anti-rabbit and goat anti-mouse IgGs (Li-Cor Bioscience, Lincoln, USA) were used as secondary antibodies, as appropriate.

2.2. Cells and viruses

RAW264.7 and human embryonic kidney (HEK293T) cells were cultured in Dulbecco's modified Eagle's medium (DMEM; Lonza Verviers, Belgium) supplemented with 10% (vol/vol) heat-inactivated fetal calf serum (FCS; Hyclone, Logan, UT, USA), 100 μg/mL of streptomycin, and 100 IU/mL of penicillin. MNV-1 (murine norovirus strain MNV-1. CW1) (Wobus et al., 2004) was kindly provided by Prof. Herbert Virgin (Department of Pathology and Immunology, Washington University School of Medicine), and produced by inoculating the virus into RAW264.7 cells. The MNV-1 cultures were purified, aliquoted, and stored at −80 °C for all subsequent experiments. The MNV-1 stock was quantified three independent times by the 50% tissue culture infective dose (TCID50).

2.3. TCID50

TCID50 assay was performed to quantify the viral titers. Briefly, 10-fold dilutions of MNV-1 were inoculated into RAW264.7 cells grown in 96-well tissue culture plate at 1,000 cells/well. The plate was incubated at 37 °C for another 5 days, followed by observing the cytopathic effect (CPE) of each well under a light scope. The TCID50 was calculated by using the Reed-Muench method.

2.4. Plasmid construction and cell transfection

The full length human RIG-I was amplified from a plasmid containing human RIG-I (kindly provided by Prof. Xuetao Cao, Nankai University, China) (Hou et al., 2014), and cloned into pcDNA3.1/Flag-HA (Addgene). The CARD domain of RIG-I was amplified and cloned into pcDNA3.1/Flag-HA and pcDNA3.1/Myc-His (kindly provided by Dr. Shuaiyang Zhao, Chinese Academy of Agricultural Sciences, China) vectors, respectively. The remaining domain of RIG-I without CARDs (pFlag-RIG-I_ΔCARD) was amplified and cloned into pcDNA3.1/Flag-HA vector. The full length and CARD domain of human MDA5 were amplified from pTRIP.CMV.IVSb.ISG.ires.TagRFP-based hMDA5 overexpression vector (kindly provided by Prof. Charles M. Rice, Rockefeller University, New York, USA) (Schoggins et al., 2011), and cloned into pcDNA3.1/Flag-HA vector. The Myc-tagged plasmid containing the CARD domain of MDA5 and the related empty vectors were kindly provided by Dr. Rei-Lin Kuo (Chang Gung University, Taiwan, China) (Kuo et al., 2019). The MNV NS7 gene was amplified from cDNA that prepared from MNV-1 infected RAW264.7 cells, and cloned into Flag- and Myc-tagged vectors, respectively (Yu et al., 2020). The related N- and C-terminus of NS7 were also amplified and cloned into Flag-tagged vectors, respectively. The pFlag-CD300lf plasmid was kindly provided by Prof. Herbert Virgin (Department of Pathology and Immunology, Washington University School of Medicine, USA) (Orchard et al., 2016). The primers used for plasmid construction are listed in Supplementary Table 1.

HEK293T cells were transfected with various plasmids at indicated concentrations using FuGENE HD Transfection Reagent (E2311; Promega) according to the manufacturer's instructions. Where necessary, the appropriate empty vectors were used to maintain a constant amount of plasmid DNA per transfection.

2.5. qRT-PCR

Total RNA was isolated with a Macherey NucleoSpin RNA II Kit (Bioke, Leiden, The Netherlands) and quantified with a Nanodrop ND-1000 (Wilmington, DE, USA). cDNA was synthesized from 500 ng of RNA using a cDNA synthesis kit (TaKaRa Bio, Inc., Shiga, Japan). The cDNA of all targeted genes were quantified by SYBR-Green-based (Applied Biosystems) real-time PCR on the StepOnePlus™ System (Thermo Fisher Scientific LifeSciences) according to the manufacturer's instructions. Human glyceraldehyde-3-phosphate dehydrogenase (GAPDH) and murine GAPDH genes were used as reference genes to normalize gene expression. The relative expression of targeted gene was calculated as $2^{-\Delta\Delta CT}$, where $\Delta\Delta C_T = \Delta C_T$sample - ΔC_Tcontrol ($\Delta C_T = C_T$[targeted gene] - C_T[GAPDH]). All primer sequences are listed in Supplementary Table 2.

2.6. Western blotting

Cultured cells were lysed in Laemmli sample buffer containing 0.1 M DTT and heated 5 min at 95 °C, then loaded onto a 10% sodium dodecyl sulfate polyacrylamide gel electrophoresis (SDS-PAGE) gel. Then proteins were further electrophoretically transferred onto a polyvinylidene difluoride (PVDF) membrane (pore size, 0.45 μM; Invitrogen) for 2 h

with an electric current of 250 mA. Subsequently, the membrane was blocked with a mixture of 2.5 mL blocking buffer (Odyssey) and 2.5 mL PBS containing 0.05% Tween 20 for 1 h, followed by overnight incubation with primary antibodies (1:1000) at 4 °C. The membrane was washed 3 times and then incubated with appropriate IRDye-conjugated secondary antibody for 1 h. After washing 3 times, protein bands were detected with the Odyssey 3.0 Infrared Imaging System (Li-Cor Biosciences).

2.7. Co-immunoprecipitation

HEK293T cells (1 X 10^5 cells/well) were co-transfected with pMyc-NS7 and pFlag-RIG-I WT, pFlag-RIG-I_CARD or pFlag-MDA5_CARD (1.5 μg/each) in 12-well tissue culture plate. At 48 h post-transfection, the cells were washed twice with cold PBS and lysed with cold NP-40 lysis buffer at 4 °C for 30 min. Halt™ Protease Inhibitor Cocktail (Thermo Fisher Scientific) was added in the lysis steps according to the manufacturer's instructions. The cells collected by scraping and lysates were cleared by centrifugation at 12,000 rpm for 10 min at 4 °C. 10% of the supernatants were taken as input control, and the remaining supernatants were incubated with a mouse anti-Flag MAb (F1804; Sigma-Aldrich) at 4 °C for 2 h, and then incubated with protein A/G plus-agarose (sc-2003; Santa Cruz) overnight at 4 °C. The agaroses were centrifuged and washed three times, and the bound proteins were analyzed by western blotting.

2.8. Confocal fluorescence microscopy

HEK293T cells (3×10^4 cells/well) were co-transfected with pFlag-RIG-I WT, pFlag-RIG-I_CARD, pFlag-MDA5 WT or pFLag-MDA5_CARD and pMyc-NS7 (1 μg/each) into μ-slide 8-well chamber (Cat. no. 80826; ibidi GmbH) for 24 h. In addition, HEK293T cells were co-transfected with pFlag-CD300lf and pMyc-RIG-I_CARD or pMyc-MDA5_CARD for 24 h, then infected with MNV-1 for 20 h. The cells were fixed with 4% paraformaldehyde in PBS, permeablized with 0.2% Triton X-100, blocked with 5% skim milk for 1 h, reacted with the appropriate antibody, and stained with 4',6-diamidino-2-phenylindole (DAPI). Antibodies used included mouse anti-Flag Mab (F1804; Sigma-Aldrich), rabbit anti-Myc Mab (71D10; Cell Signaling), mouse anti-Myc Mab (9B11; Cell Signaling), rabbit anti-NS7 antisera, and anti-rabbit IgG (H+L), F(ab')2 Fragment (Alexa Fluor® 488 and 594 conjugate) or anti-mouse IgG(H+L), F(ab') 2 Fragment (Alexa Fluor 488 and 594 conjugate) secondary antibodies. Imaging was performed on a Leica SP5 confocal microscopy using a 63x oil objective.

2.9. Antiviral assay with MNV

HEK293T cells (8×10^4 cells/well) were co-transfected with pFlag-CD300lf and pFlag-RIG-I_WT, pFlag-RIG-I_CARD, pFlag-MDA5_WT, or pFlag-MDA5_CARD with indicated concentrations in 24-well tissue culture plate for 24 h, then infected with MNV-1 for 20 h. The total RNA, supernatants and protein samples were collected and used for determination of antiviral activity of RIG-I and MDA5. To determine whether MNV NS7 could regulate RLRs-mediated antiviral response, HEK293T cells were co-transfected with pFlag-CD300lf and pFlag-RIG-I_WT, pFlag-RIG-I_CARD, pFlag-MDA5_WT, pFlag-MDA5_CARD, or pFlag-NS7 for 24 h, followed with infection of MNV-1 for 20 h. The total RNA and protein samples were collected for further analysis.

2.10. Statistical analysis

Data are presented as the mean ± SEM. Comparisons between groups were performed with Mann-Whitney test using GraphPad Prism 5.0 (GraphPad Software Inc., La Jolla, CA, USA). Differences were considered significant at a P value less than 0.05.

3. Results

3.1. MNV NS7 enhances RIG-I triggered IFN response

To examine the effects of MNV RdRp on IFN response, we first tested in the context of poly (I:C) triggered IFN response. We found that viral NS7 alone did not affect IFN-β transcription, but enhanced poly (I:C) triggered IFN-β transcription (Supplementary Fig. 1A) and transcription of ISGs including IFIT1 and IFIT3 (Supplementary Fig. 1B). Besides TLR3, RIG-I and MDA5 have been implicated in the recognition of poly (I:C) and the subsequent induction of IFN response (Kato et al., 2006; Yoneyama et al., 2005). To investigate whether MNV NS7 could regulate RIG-I-mediated IFN signaling, HEK293T cells were co-transfected with pFlag-RIG-I_WT and pFlag-NS7 for 24 h (Fig. 1A). We found that NS7 overexpression alone did not trigger IFN response, but enhanced RIG-I induced IFN-β transcription (Fig. 1B), as well as the downstream ISG transcription (Fig. 1C). It has been reported that the CARDs of RIG-I are responsible for signal transduction and activation of IRF-3 and NF-κB, as well as subsequent IFN response (Yoneyama et al., 2004). Thus, we constructed the truncated RIG-I domains (Fig. 1D) and further investigated whether NS7 also augments RIG-I_CARD and RIG-I_ΔCARD triggered IFN activation. We found that RIG-I_CARD induced IFN-β and ISG transcription were enhanced by NS7 (Fig. 1E and 1F). The helicase domain of RIG-I (RIG-I_ΔCARD) has been reported to have negative regulatory effects by blocking newcastle disease virus-induced IRF3 activation (Yoneyama et al., 2004). Consistently, we found RIG-I_ΔCARD did not trigger IFN activation, which was also not further triggered by NS7 (Fig. 1E and 1F). These results demonstrated that MNV NS7 positively regulates RIG-I mediated IFN signaling.

3.2. Interaction and co-localization of MNV NS7 with RIG-I

It has been reported that the replicases of EV71 and CVB3 inhibit MDA5 triggered IFN signaling through interaction with the CARDs of MDA5 (Kuo et al., 2019). This prompted us to investigate whether there is an interaction between NS7 and RIG-I. HEK293T cells were co-transfected with Flag-tagged RIG-I and Myc-tagged NS7 for 48 h. The lysates of transfected cells were subjected to immunoprecipitation by anti-Flag resin, and our results showed that RIG-I could precipitate with NS7 protein (Fig. 2A). As aforementioned, the CARDs of RIG-I is able to activate the IFN response, which is further increased by MNV NS7 expression (Fig. 1F). We further demonstrated the interaction between NS7 and RIG-I_CARD in HEK293T cells co-transfected with Flag-tagged RIG-I_CARD and Myc-tagged NS7 (Fig. 2B). Moreover, we examined the localization of NS7 with RIG-I proteins in cells. Confocal microscopy revealed that besides nucleus localization, MNV NS7 could co-localize with either RIG-I or the CARDs of RIG-I in the cytoplasm (Fig. 2C). These data demonstrated that MNV NS7 interacts with RIG-I and its N-terminus (CARDs), and this interaction might explain the augment of RIG-I mediated IFN activation by NS7.

3.3. NS7 interacts with MDA5 and enhances MDA5 triggered ISG transcription

Next, we examined the effect of MNV NS7 on another RLR, MDA5. We co-transfected the pTRIP.CMV.IVSb.ISG.ires.TagRFP-MDA5 and pFlag-NS7 into HEK293T cells for 24 h, and found that NS7 overexpression enhanced MDA5 induced IFN-β transcription (Fig. 3A). Because the CARDs of MDA5 alone could initiate IFN activation and ISG transcription (Kuo et al., 2019), we further determined whether NS7 could trigger MDA5_CARD mediated IFN response. We co-transfected the Myc-tagged MDA5_CARD and NS7 into HEK293T cells (Fig. 3B), and found that IFN-β transcription activated by MDA5_CARD was further increased by co-expression of MNV NS7 (Fig. 3C). Consistently, this effect was also observed on the induction of downstream antiviral ISGs including IFIT1 and IFIT3 (Fig. 3C). Similar to the interaction with

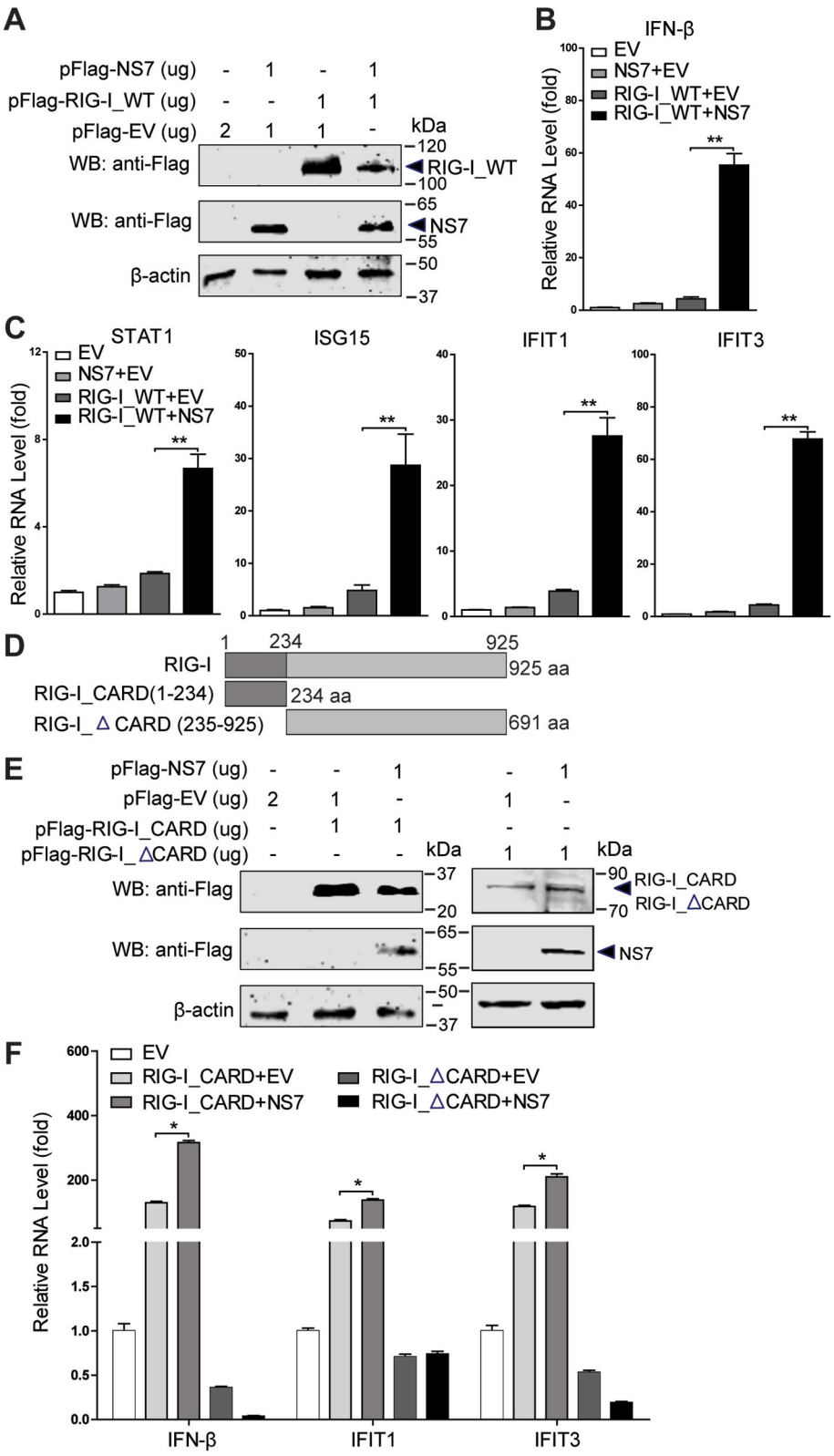

Fig. 1. MNV NS7 enhances RIG-I triggered IFN response. HEK293T cells were transfected with pFlag-RIG-I_WT, pFlag-NS7, or empty vectors with indicated concentrations for 24 h. (A) The protein expression of transfected vectors was analyzed by western blotting. (B) The IFN-β mRNA level was analyzed by qRT-PCR assay (n = 6). (C) The mRNA levels of STAT1, ISG15, IFIT1 and IFIT3 were analyzed by qRT-PCR assay (n = 6). (D) Schematic representation of truncated RIG-I domains. HEK293T cells were transfected with pFlag-RIG-I_CARD, pFlag-RIG-I_ΔCARD, or empty vectors with indicated concentrations for 24 h. (E) The protein expression of transfected vectors was analyzed by western blotting. (F) The mRNA levels of IFN-β, IFIT1 and IFIT3 were analyzed by qRT-PCR assay (n = 4–8). Data (B, C and F) were normalized to the EV control (set as 1). *P < 0.05; **P < 0.01. β-actin was used as a loading control.

the CARDs of RIG-I, we found that NS7 also interacts with the CARDs of MDA5 (Fig. 3D). Furthermore, we also investigated the localization of NS7 with MDA5 proteins in HEK293T cells by confocal microscopy. The results showed the expression and localization of Flag-tagged MDA5 and its CARDs in the cytoplasm (Fig. 3E), which also co-localized with MNV NS7 in the cytoplasm, while NS7 also diffused in the nucleus (Fig. 3F).

We next investigated whether the N- or C-terminus of NS7 are responsible for the effects on RIG-I and MDA5 mediated IFN activation. The N- or C-terminus of NS7 with Flag tag were constructed (Supplementary Fig. 2A and 2B). HEK293T cells were co-transfected with Flag-tagged CARDs of RIG-I or MDA5, and N- or C-terminus of NS7. At 24 h post-transfection, we found that the upregulation of IFN-β, IFIT1 and

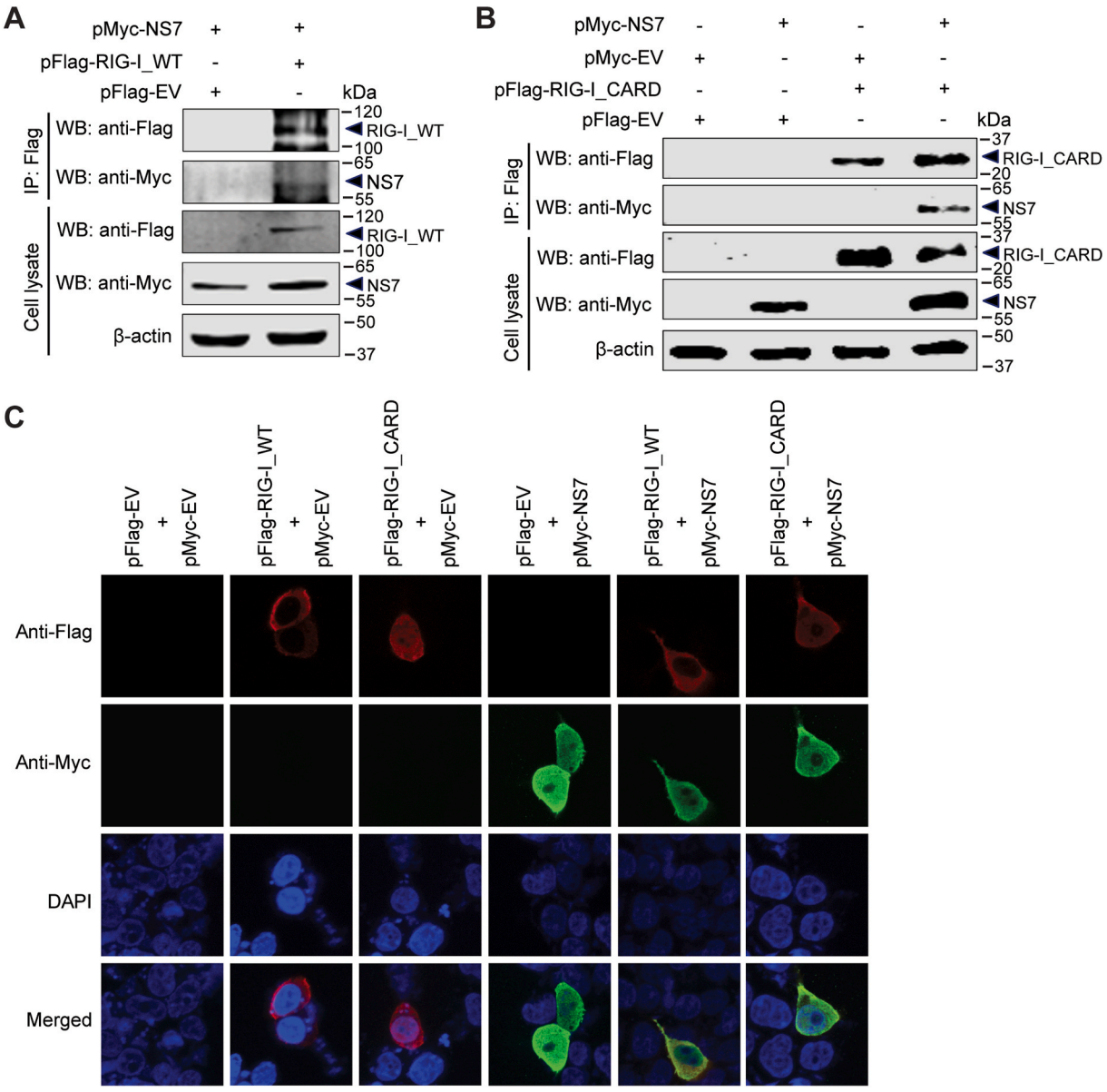

Fig. 2. Interaction and co-localization of MNV NS7 with RIG-I. (A) HEK293T cells were transfected with pMyc-NS7 (1.5 μg) and pFlag-RIG-I_WT (1.5 μg), or empty vectors for 48 h. Co-IP was performed using anti-Flag MAb (1:1000). The precipitated proteins were analyzed by western blotting using antibodies against the Flag and Myc tags. (B) HEK293T cells were transfected with pMyc-NS7 (1.5 μg) and pFlag-RIG-I_CARD (1.5 μg), or empty vectors for 48 h. Co-IP was performed using anti-Flag MAb (1:1000). The precipitated proteins were analyzed by western blotting using antibodies against the Flag and Myc tags. (C) Co-localization of RIG-I and RIG-I_CARD with NS7. Expression plasmids pMyc-NS7 and pFlag-RIG-I_WT, pFlag-RIG-I_CARD, or empty vectors (1 μg/each) were transfected into HEK293T cells for 24 h and then subjected to a confocal assay. β-actin was used as a loading control.

IFIT3 transcription triggered by CARDs of RIG-I or MDA5 was slightly enhanced by N-terminus of NS7 (Supplementary Fig. 2C and 2D). The C-terminus of NS7 appeared not to affect RIG-I_CARD but inhibited MDA5_CARD mediated IFN activation (Supplementary Fig. 2C and 2D). These results collectively suggested that the intact of MNV NS7 is essential for effective augmentation of RIG-I and MDA5 mediated IFN activation.

3.4. Co-localization of NS7 with the CARDs of RIG-I and MDA5 in MNV infected human cells

Ectopic expression of the MNV receptor mouse CD300lf breaks the species barriers for MNV infection in human cells (Orchard et al., 2016). Thus, we determined MNV replication by immunoblotting viral NS1/2 protein in human HEK293T cells that were transfected with Flag-tagged CD300lf and infected with the virus (Fig. 4A). In addition, we confirmed viral replication by targeting viral NS7 protein with rabbit anti-NS7 antisera using confocal microscopy (Fig. 4B). We next examined co-localization of MNV NS7 with the CARDs of RIG-I and MDA5 in infected cells. In order to avoid the influence by the Flag tag of MNV receptor, we co-transfected the pFlag-CD300lf with pMyc-RIG-I_CARD or pMyc-MDA5_CARD into HEK293T cells for 24 h (Fig. 4C), then infected with MNV-1 for 20 h. The results showed that besides nucleus localization, MNV NS7 can co-localize with the CARDs of RIG-I and MDA5 in the cytoplasm of infected cells (Fig. 4D), which is in accordance with previous studies demonstrating the diffuse of NS7 protein in the cytoplasm and nuclear in infected cells (Hyde et al., 2009). The activator of TLR3 signaling, poly (I:C) triggers IFN response involving RIG-I and MDA5 activation. Thus, we used poly (I:C) to activate the endogenous RIG-I and MDA5, and confirmed co-localization of RIG-I

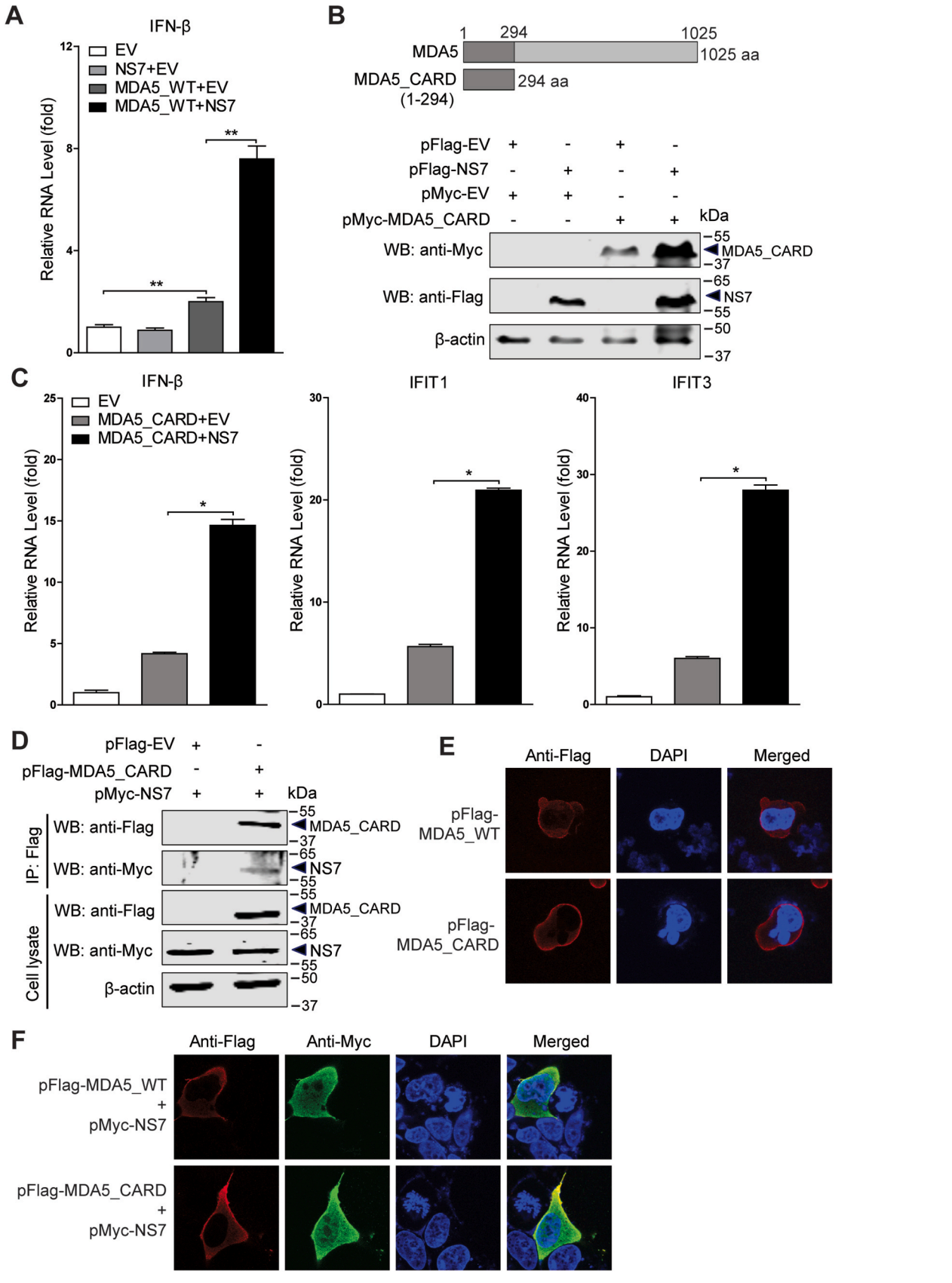

(caption on next page)

Fig. 3. NS7 interacts with MDA5 and enhances MDA5 triggered ISG transcription. (A) qRT-PCR analysis of IFN-β mRNA level in HEK293T cells that were transfected with pFlag-NS7, pFLuc-MDA5, or empty vectors (1 μg/each) for 24 h (n = 6). (B) Schematic representation of CARD domain of MDA5. HEK293T cells were transfected with pFlag-NS7, pMyc-MDA5_CARD, or empty vectors (1 μg/each) for 24 h. Western blotting analysis of the expression of indicated transfected vectors. (C) The mRNA levels of IFN-β, IFIT1 and IFIT3 were analyzed by qRT-PCR assay (n = 4). (D) HEK293T cells were transfected with pMyc-NS7 (1.5 μg) with pFlag-MDA5_CARD (1.5 μg), or empty vectors for 48 h. Co-IP was performed using anti-Flag MAb (1:1000). The precipitated proteins were analyzed by western blotting using antibodies against the Flag and Myc tags. (E) Confocal analysis of expression and localization of MDA5 and MDA5_CARD in HEK293T cells that were transfected with pFlag-MDA5_WT and pFlag-MDA5_CARD (1 μg/each) for 24 h. (F) Co-localization of MDA5 or MDA5_CARD with NS7. Expression plasmids pMyc-NS7 and pFlag-MDA5_WT, or pFlag-MDA5_CARD (1 μg/each) were transfected into HEK293T cells for 24 h and then subjected to a confocal assay. Data (A and C) were normalized to the EV control (set as 1). *P < 0.05; **P < 0.01. β-actin was used as a loading control.

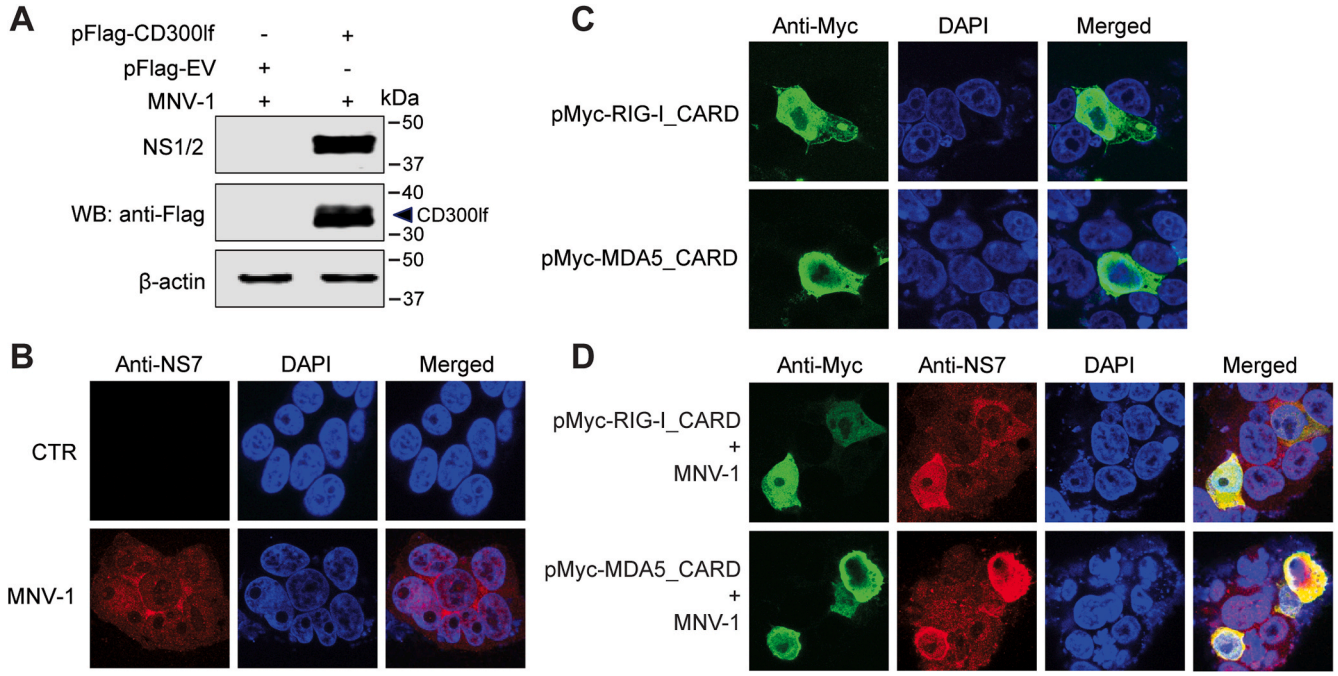

Fig. 4. Co-localization of viral NS7 with the CARDs of RIG-I and MDA5 in MNV infected human cells. (A) HEK293T cells were transfected with pFlag-CD300lf (1 μg) or empty vectors (1 μg) for 24 h, then infected with MNV-1 for 20 h. Expression of viral NS1/2 protein and the transfected vectors were analyzed by western blotting. (B) HEK293T cells were transfected with pFlag-CD300lf (1 μg) for 24 h, then uninfected or infected with MNV-1 for 20 h. Expression of viral NS7 protein was analyzed by confocal assay. (C) HEK293T cells were transfected with pMyc-RIG-I_CARD (1 μg) or pMyc-MDA5_CARD (1 μg) for 24 h. The expression and localization of RIG-I_CARD and MDA5_CARD were analyzed by confocal assay. (D) HEK293T cells were transfected with pFlag-CD300lf (0.5 μg) and pMyc-RIG-I_CARD (1 μg) or pMyc-MDA5_CARD (1 μg) for 24 h, then infected with MNV-1 for 20 h. Co-localization of RIG-I_CARD or MDA5_CARD with NS7 in MNV-1 infected cells was analyzed by confocal assay.

(Supplementary Fig. 3A) and MDA5 (Supplementary Fig. 3B) with viral NS7 in MNV-infected HEK293T cells. In addition, we found anti-MNV effects of poly (I:C) in HEK293T cells expressing MNV receptor (Supplementary Fig. 3C).

3.5. *RIG-I and MDA5 restrict MNV replication, which is augmented by NS7 overexpression*

We evaluated the anti-MNV activity of RIG-I and MDA5 in HEK293T cells. We found that RIG-I overexpression inhibited MNV infection in CD300lf transduced HEK293T cells, as shown at both viral RNA (Fig. 5A) and NS1/2 protein level (Fig. 5B). Consistently, the CARDs of RIG-I exerted similar inhibitory effects (Fig. 5C). Moreover, the viral titers were also decreased by RIG-I CARDs overexpression (Fig. 5F). Similar results were observed for the N-terminus and full-length of MDA5 (Fig. 5D-F).

JAK/STAT cascade is a key component of the IFN signaling. Thus, we examined whether blocking JAK/STAT pathway would affect RIG-I and MDA5 mediated antiviral activity. HEK293T cells were co-transfected with pFlag-CD300lf and pFlag-RIG-I_CARD, or pFlag-MDA5_CARD for 20 h, treated with JAK inhibitor 1 for 6 h, and then infected with MNV-1 for 20 h. We found the inhibitory effects on viral RNA by CARDs of RIG-I or and MDA5 were partially reversed by JAK inhibitor, respectively (Fig. 6A). Consistently, the induction of IFN-β, IFIT1 and IFIT3 transcription was also attenuated (Fig. 6B and 6C). These results showed that the anti-MNV activity of RIG-I and MDA5 requires activation of the JAK/STAT pathway.

In HEK293T cells, overexpression of NS7 did not affect viral NS1/2 protein expression (Supplementary Fig. 2E). Thus, we examined the effects of MNV NS7 on RIG-I mediated anti-MNV ability, by co-transfecting HEK293T cells with Flag-tagged CD300lf, RIG-I or its CARDs and NS7 for 24 h, and then infected with MNV-1 for 20 h. The results showed that NS7 enhanced RIG-I or CARDs of RIG-I mediated inhibition of viral RNA (Fig. 7A and 7B). Similar effects were observed for MDA5 (Fig. 7C and 7D). Interestingly, the N- or C-terminus of NS7 overexpression also did not affect viral NS1/2 protein expression (Supplementary Fig. 2E), and the CARDs of RIG-I and MDA5 mediated inhibition of viral RNA (Supplementary Fig. 2F and 2G). These results revealed that the intact version of MNV NS7 enhances the anti-MNV activity of RIG-I and MDA5.

4. Discussion

Numerous studies have reported that viruses explore different strategies to counteract host antiviral defense. By striking contract, our results demonstrated that MNV RdRp promotes host antiviral response.

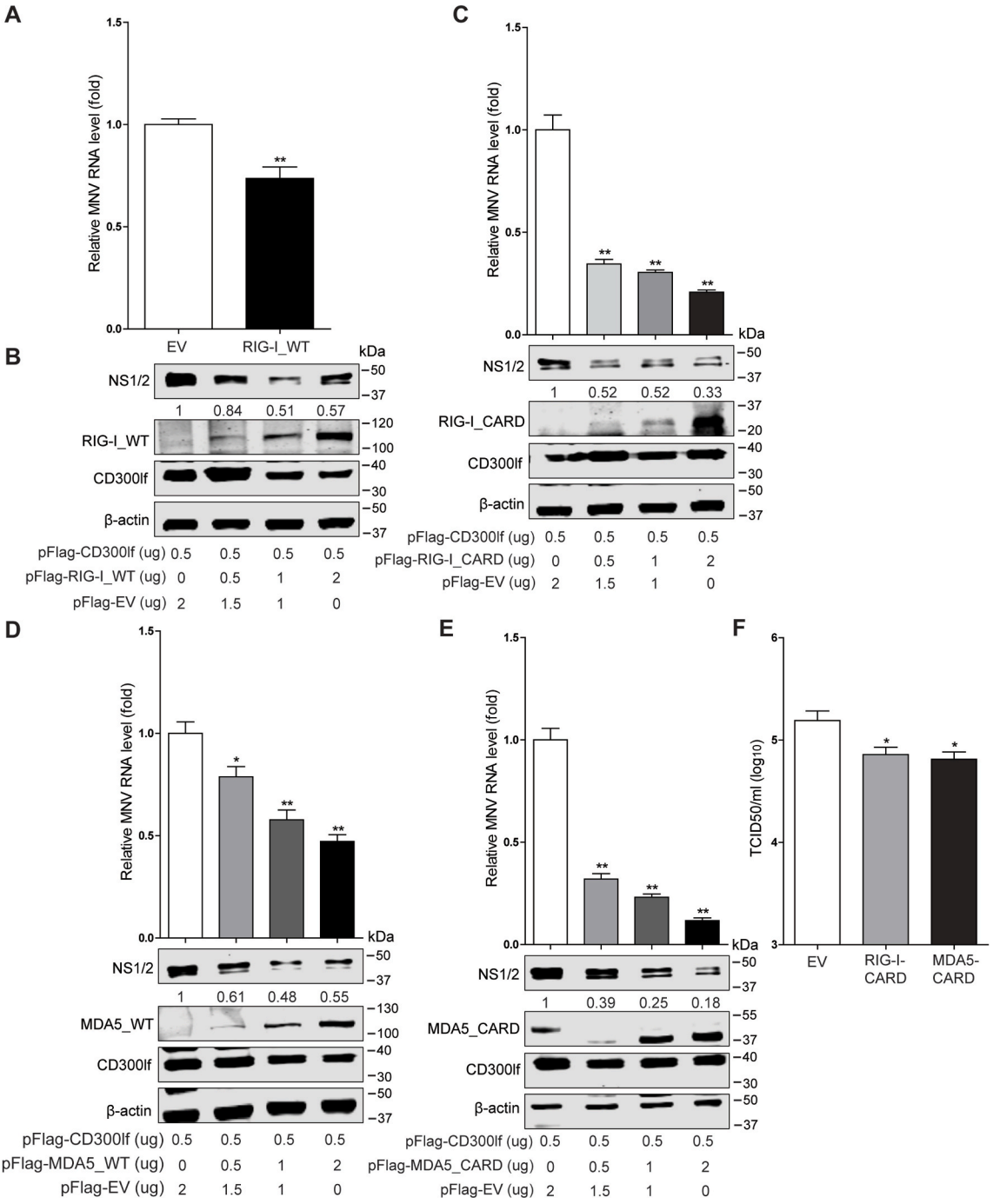

Fig. 5. RIG-I or MDA5 overexpression restricts MNV replication. (A) HEK293T cells were transfected with pFlag-CD300lf (0.5 μg) and pFlag-RIG-I_WT (1 μg), or empty vectors (1 μg) for 24 h, then infected with MNV-1 for 20 h. The viral RNA level was analyzed by qRT-PCR assay (n = 6). (B) HEK293T cells were transfected with pFlag-CD300lf and pFlag-RIG-I_WT, or empty vectors with indicated concentrations for 24 h, then infected with MNV-1 for 20 h. The expression of viral NS1/2 and transfected vectors was analyzed by western blotting. (C) HEK293T cells were transfected with pFlag-CD300lf and pFlag-RIG-I_CARD, or empty vectors with indicated concentrations for 24 h, then infected with MNV-1 for 20 h. The viral RNA level, and the expression of viral NS1/2 and transfected vectors were analyzed by qRT-PCR (n = 6) and western blotting, respectively. (D) HEK293T cells were transfected with pFlag-CD300lf and pFlag-MDA5_WT, or empty vectors with indicated concentrations for 24 h, then infected with MNV-1 for 20 h. The viral RNA level, and the expression of viral NS1/2 and transfected vectors were analyzed by qRT-PCR (n = 6) and western blotting, respectively. (E) HEK293T cells were transfected with pFlag-CD300lf and pFlag-MDA5_CARD, or empty vectors with indicated concentrations for 24 h, then infected with MNV-1 for 20 h. The viral RNA level, and the expression of viral NS1/2 and transfected vectors were analyzed by qRT-PCR (n = 6) and western blotting, respectively. (F) HEK293T cells were transfected with pFlag-CD300lf (0.5 μg) and pFlag-RIG-I_CARD (2 μg), pFlag-MDA5_CARD (2 μg), or empty vectors (2 μg) for 24 h, then infected with MNV-1 for 20 h. The viral titer was analyzed by TCID50 assay (n = 6). Data (A, C, D, E, and F) were normalized to the EV control (set as 1). *P < 0.05; **P < 0.01. β-actin was used as a loading control. For immunoblot results (B, C, D and E), band intensity of NS1/2 protein in each lane was quantified by Odyssey software, and the quantification results were normalized to β-actin expression (EV control, set as 1).

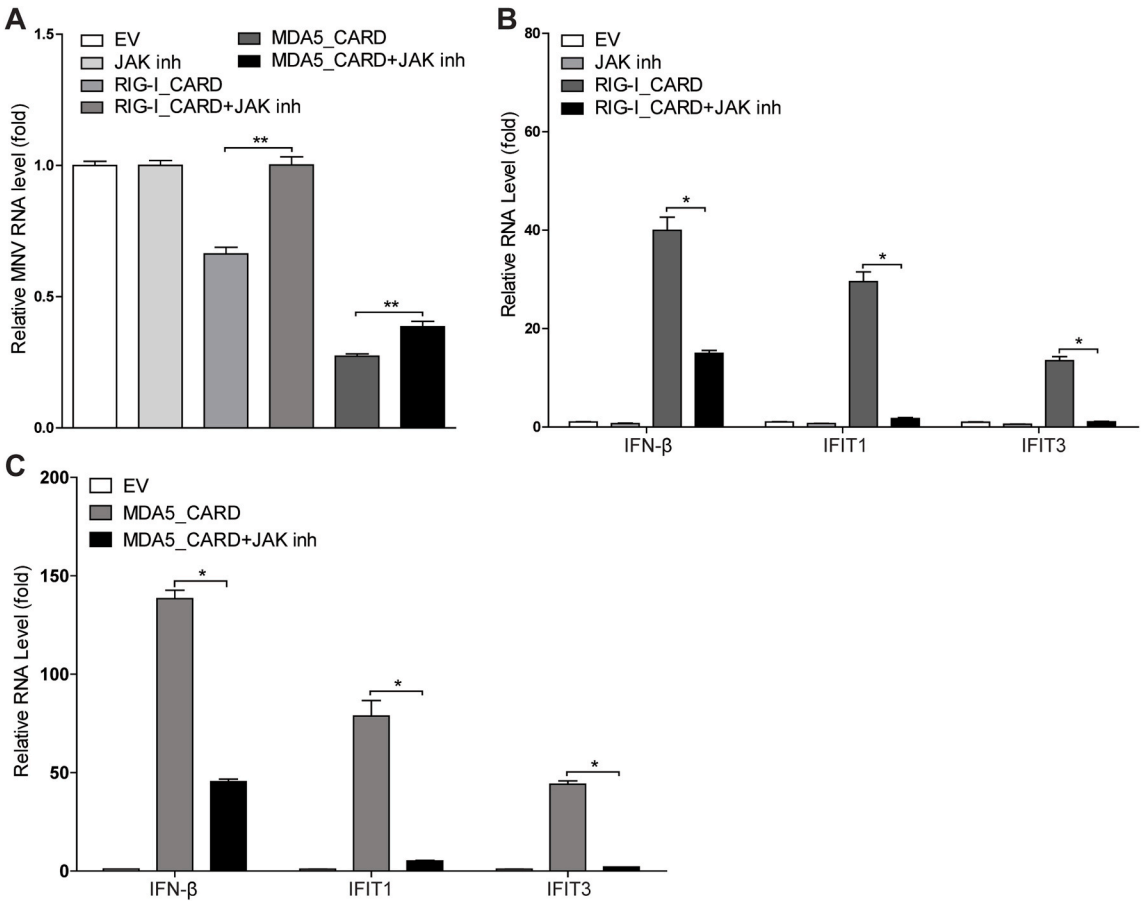

Fig. 6. Anti-MNV activity of RIG-I and MDA5 requires activation of the JAK/STAT pathway. HEK293T cells were transfected with pFlag-CD300lf (0.5 μg) and pFlag-RIG-I_CARD (1 μg), or pFlag-MDA5_CARD (1 μg) for 20 h, then treated with JAK inhibitor 1 (5 mM) for 6 h, then infected with MNV-1 for 20 h. The viral RNA levels (A) were analyzed by qRT-PCR (n = 6). HEK293T cells were transfected with (B) pFlag-RIG-I_CARD (1 μg), or (C) pFlag-MDA5_CARD (1 μg) for 20 h, then treated with JAK inhibitor 1 (5 mM) for 6 h. The mRNA level of IFN-β, IFIT1 and IFIT3 were analyzed by qRT-PCR (n = 4). Data (A) were normalized to the EV and JAK inh control (both set as 1). Data (B and C) were normalized to the EV control (set as 1). *P < 0.05; **P < 0.01.

Although NS7 alone does not affect IFN signaling, it potently enhances RIG-I and MDA5 triggered antiviral IFN response.

RIG-I and MDA5 can recognize dsRNA or 5′-pppRNA in the cytoplasm to induce downstream IFN signaling. MNV has been reported to be recognized by MDA5 and activate IFN signaling in mouse macrophages (Emmott et al., 2017; McCartney et al., 2008). Although the main function of viral replicases is to drive viral replication and transcription, different regulatory functions of viral replicases on RLRs-mediated IFN signaling have been reported (Kuo et al., 2019; Miller et al., 2020; Moriyama et al., 2007; Nikonov et al., 2013; Painter et al., 2015; Subba-Reddy et al., 2011). Previous studies have revealed that MNV RdRp upregulates RIG-I mediated IFN-β promotor activation (Subba-Reddy et al., 2011). Our results have demonstrated that MNV NS7 can augment both RIG-I and MDA5 mediated IFN antiviral response. The mechanism of assisting RLRs-mediated IFN response by viral replicases has been linked to the conversion or modification of host RNA into dsRNA (Nikonov et al., 2013; Yu et al., 2012). In contrast, inhibition of MDA5 triggered IFN activation by enteroviral replicases has been reported through direct protein-protein interactions (Kuo et al., 2019). In this study, we demonstrated that MNV NS7 interacts with the CARDs of RIG-I and MDA5. These interactions may explain the augmentation of RLRs-mediated IFN activation by MNV NS7, although further studies are needed to provide definitive proof.

Toll-like receptors (TLRs) including TLR3, TLR7 and TLR8 are essential for activation of antiviral response upon viral infection, and can sense ssRNA or dsRNA in the cytosol (Jensen and Thomsen, 2012). Studies have shown a slight increase of MNV viral titers in TLR3 deficient mice (McCartney et al., 2008). Although HuNV RdRp does not enhance TLR3-mediated IFN-β promoter activation (Subba-Reddy et al., 2011), we found that MNV NS7 increased the transcription of several ISGs triggered by poly (I:C). Besides RIG-I and MDA5 associated with poly (I:C) triggered IFN response, poly (I:C) is also the activator of TLR3 signaling. Thus, it is interesting to further investigate whether there is a regulatory role of MNV NS7 on TLRs-mediated IFN response.

Studies have shown that MNV-1 replicates to higher levels in MDA5 deficient mice (McCartney et al., 2008), but HuNV replication is not affected by silencing RIG-I signaling (Guix et al., 2007). We have previously demonstrated that ectopic expression of RIG-I and MDA5 potently inhibit HuNV replication in the HG23 replicon model (Dang et al., 2018). In this study, we demonstrated that RIG-I and MDA5 exert antiviral activity against MNV replication in human cells ectopically expressing MNV receptor. ISGs are considered as the ultimate antiviral effectors, and the essential role of STAT1 in controlling MNV replication has been demonstrated (Karst et al., 2003). By blocking the JAK/STAT pathway, the CARDs of RIG-I and MDA5 mediated ISG transcription and anti-MNV activity are partially attenuated, suggesting the requirement of JAK/STAT pathway for RLRs-mediated antiviral actions. We also revealed that NS7 overexpression enhances RIG-I and MDA5 mediated inhibition of viral RNA, consistent with the augmentation of IFN response.

In summary, we demonstrated that MNV NS7 interacts with the N-terminus of RIG-I and MDA5 and enhances RIG-I and MDA5 triggered IFN response. Furthermore, RIG-I and MDA5 potently inhibit MNV replication requiring the activation of JAK/STAT pathway, and this

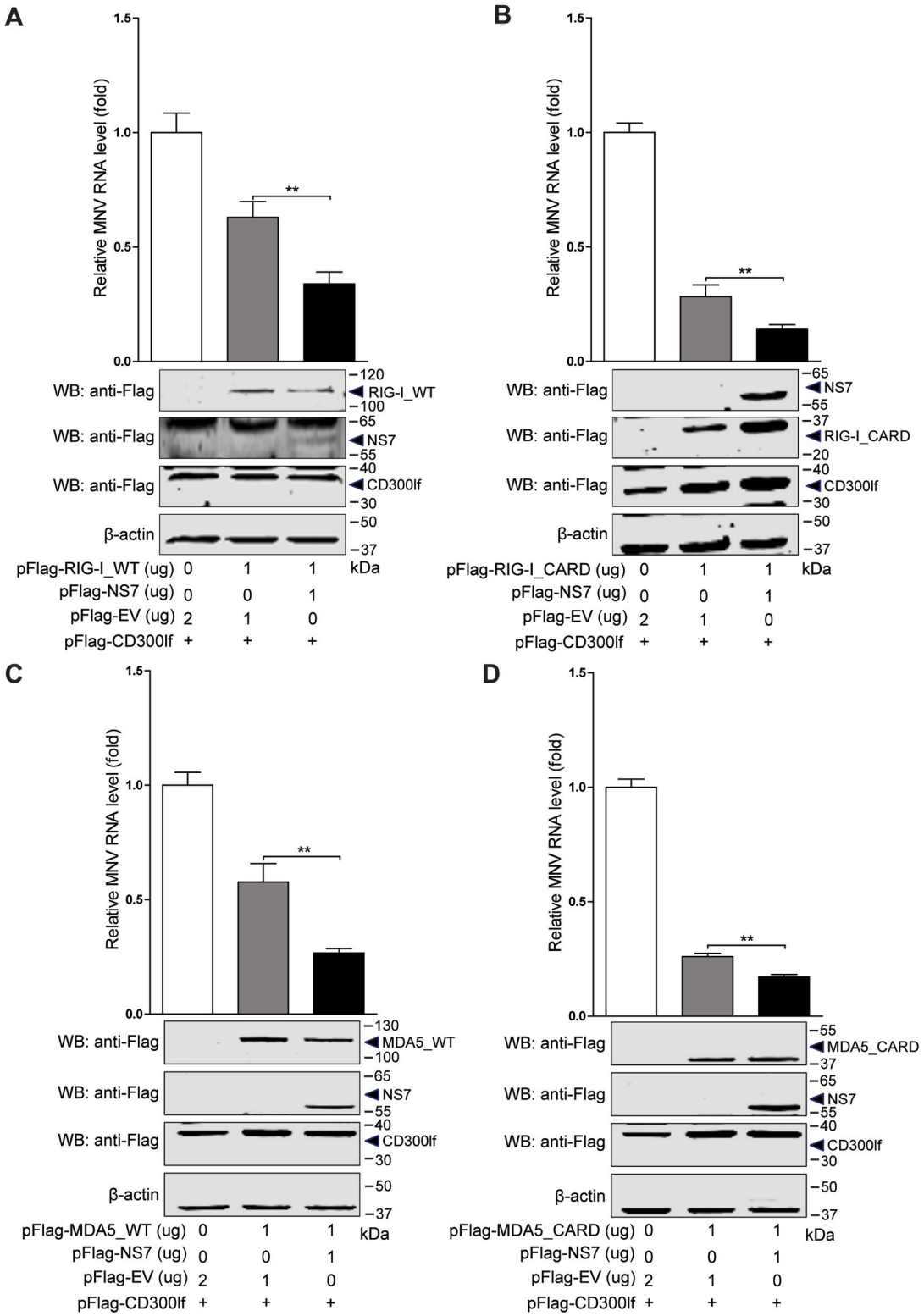

Fig. 7. NS7 enhances RLRs-mediated inhibition of MNV RNA replication. (A) HEK293T cells were transfected with pFlag-CD300lf (0.5 μg) and pFlag-RIG-I_WT, pFlag-NS7, or empty vectors with indicated concentrations for 24 h, then infected with MNV-1 for 20 h. The viral RNA level and the expression of transfected vectors were analyzed by qRT-PCR (n = 6–9) and western blotting, respectively. (B) HEK293T cells were transfected with pFlag-CD300lf (0.5 μg) and pFlag-RIG-I_CARD, pFlag-NS7, or empty vectors with indicated concentrations for 24 h, then infected with MNV-1 for 20 h. The viral RNA level and expression of transfected vectors were analyzed by qRT-PCR (n = 7–9) and western blotting, respectively. (C) The expression vector pFlag-CD300lf (0.5 μg) and pFlag-MDA5_WT, pFlag-NS7, or empty vectors were transfected into HEK293T cells with indicated concentrations for 24 h, then infected with MNV-1 for 20 h. The viral RNA level and expression of transfected vectors were analyzed by qRT-PCR (n = 4–6) and western blotting, respectively. (D) The expression vector pFlag-CD300lf (0.5 μg) and pFlag-MDA5_CARD, pFlag-NS7, or empty vectors were transfected into HEK293T cells with indicated concentrations for 24 h, then infected with MNV-1 for 20 h. The viral RNA level and expression of transfected vectors were analyzed by qRT-PCR (n = 7–9) and western blotting, respectively. Data were normalized to the EV control (set as 1). **P < 0.01. β-actin was used as a loading control.

antiviral effect is augmented by NS7. We postulate that MNV has developed sophisticated strategies to efficiently replicate but also survive in the host cells. At the early stage of infection, viral proteins such as VF1 and VP2 can regulate cellular immune response to facilitate viral replication (McFadden et al., 2011; Zhu et al., 2013). In contrast, NS7 as a RdRp can sensitively recognize the level of viral replication. As a feedback reaction, NS7 can interact and augment RIG-I and MDA5 mediated antiviral IFN response to inhibit over-replication, and thus protect host cells from lysis in order to survive in the host. However, future experimental studies are required to further validate this theory. Furthermore, augmentation of antiviral response by MNV NS7 may have an impact on superinfection of other pathogens, as different pathogens cohabit in the intestine. Thus, this aspect is interesting to be further investigated.

Declaration of competing interest

The authors declare that they have no competing interests.

Acknowledgements

We gratefully acknowledge Prof. Herbert W. Virgin (Washington University, St Louis, MO, USA) for providing us the MNV-1 and Flag-tagged CD300lf plasmid; Prof. Vernon K. Ward (School of Biomedical Sciences, University of Otago, New Zealand) for providing rabbit polyclonal antisera to MNV NS1/2; Prof. Ian Goodfellow (Department of Pathology, University of Cambridge, UK) for providing rabbit polyclonal antisera to MNV NS7; Dr. Shuaiyang Zhao (Chinese Academy of Agricultural Sciences, China) for providing the pcDNA3.1/Myc-His vector; Dr. Rei-Lin Kuo (Chang Gung University, Taiwan, China) for providing the pMyc-MDA5_CARD and the related empty vectors; Prof. Xuetao Cao (Nankai University, China) for providing Flag-tagged human RIG-I plasmid; Prof. Charles M. Rice (Rockefeller University, USA) for providing pTRIP.CMV.IVSb.ISG.ires.TagRFP-based human MDA5 plasmid. This research is supported by the Netherlands Organization for Scientific Research (NWO) for a VIDI grant (No. 91719300) to Q. Pan, and by the China Scholarship Council for funding PhD fellowships to P. Yu (No. 201708620177), Y. Li (No. 201703250073), Y. Li (No. 201708530243), Z. Miao (No. 201708530234) and Y. Wang (No. 201903250082).

Appendix A. Supplementary data

Supplementary data to this article can be found online at https://doi.org/10.1016/j.antiviral.2020.104877.

References

Bok, K., Green, K.Y., 2012. Norovirus gastroenteritis in immunocompromised patients. N. Engl. J. Med. 367, 2126–2132.
Dang, W., Xu, L., Yin, Y., Chen, S., Wang, W., Hakim, M.S., Chang, K.O., Peppelenbosch, M.P., Pan, Q., 2018. IRF-1, RIG-I and MDA5 display potent antiviral activities against norovirus coordinately induced by different types of interferons. Antivir. Res. 155, 48–59.
Davies, C., Brown, C.M., Westphal, D., Ward, J.M., Ward, V.K., 2015. Murine norovirus replication induces G0/G1 cell cycle arrest in asynchronously growing cells. J. Virol. 89, 6057–6066.
Emmott, E., de Rougemont, A., Hosmillo, M., Lu, J., Fitzmaurice, T., Haas, J., Goodfellow, I., 2019. Polyprotein processing and intermolecular interactions within the viral replication complex spatially and temporally control norovirus protease activity. J. Biol. Chem. 294, 4259–4271.
Emmott, E., Sorgeloos, F., Caddy, S.L., Vashist, S., Sosnovtsev, S., Lloyd, R., Heesom, K., Locker, N., Goodfellow, I., 2017. Norovirus-mediated modification of the translational landscape via virus and host-induced cleavage of translation initiation factors. Mol. Cell. Proteomics 16, S215–S229.
Glass, R.I., Parashar, U.D., Estes, M.K., 2009. Norovirus gastroenteritis. N. Engl. J. Med. 361, 1776–1785.
Guix, S., Asanaka, M., Katayama, K., Crawford, S.E., Neill, F.H., Atmar, R.L., Estes, M.K., 2007. Norwalk virus RNA is infectious in mammalian cells. J. Virol. 81, 12238–12248.
Högbom, M., Jäger, K., Robel, I., Unge, T., Rohayem, J., 2009. The active form of the norovirus RNA-dependent RNA polymerase is a homodimer with cooperative activity. J. Gen. Virol. 90, 281–291.
Honda, K., Takaoka, A., Taniguchi, T., 2006. Type I interferon [corrected] gene induction by the interferon regulatory factor family of transcription factors. Immunity 25, 349–360.
Hou, J., Zhou, Y., Zheng, Y., Fan, J., Zhou, W., Ng, I.O., Sun, H., Qin, L., Qiu, S., Lee, J. M., Lo, C.M., Man, K., Yang, Y., Yang, Y., Yang, Y., Zhang, Q., Zhu, X., Li, N., Wang, Z., Ding, G., Zhuang, S.M., Zheng, L., Luo, X., Xie, Y., Liang, A., Wang, Z., Zhang, M., Xia, Q., Liang, T., Yu, Y., Cao, X., 2014. Hepatic RIG-I predicts survival and interferon-alpha therapeutic response in hepatocellular carcinoma. Canc. Cell 25, 49–63.
Hyde, J.L., Gillespie, L.K., Mackenzie, J.M., 2012. Mouse norovirus 1 utilizes the cytoskeleton network to establish localization of the replication complex proximal to the microtubule organizing center. J. Virol. 86, 4110–4122.
Hyde, J.L., Sosnovtsev, S.V., Green, K.Y., Wobus, C., Virgin, H.W., Mackenzie, J.M., 2009. Mouse norovirus replication is associated with virus-induced vesicle clusters originating from membranes derived from the secretory pathway. J. Virol. 83, 9709–9719.
Jensen, S., Thomsen, A.R., 2012. Sensing of RNA viruses: a review of innate immune receptors involved in recognizing RNA virus invasion. J. Virol. 86, 2900–2910.
Karst, S.M., Wobus, C.E., Goodfellow, I.G., Green, K.Y., Virgin, H.W., 2014. Advances in norovirus biology. Cell Host Microbe 15, 668–680.
Karst, S.M., Wobus, C.E., Lay, M., Davidson, J., Virgin, H.W., 2003. STAT1-dependent innate immunity to a Norwalk-like virus. Science 299, 1575–1578.
Kato, H., Takeuchi, O., Sato, S., Yoneyama, M., Yamamoto, M., Matsui, K., Uematsu, S., Jung, A., Kawai, T., Ishii, K.J., Yamaguchi, O., Otsu, K., Tsujimura, T., Koh, C.S., Reis e Sousa, C., Matsuura, Y., Fujita, T., Akira, S., 2006. Differential roles of MDA5 and RIG-I helicases in the recognition of RNA viruses. Nature 441, 101–105.
Kawai, T., Takahashi, K., Sato, S., Coban, C., Kumar, H., Kato, H., Ishii, K.J., Takeuchi, O., Akira, S., 2005. IPS-1, an adaptor triggering RIG-I- and Mda5-mediated type I interferon induction. Nat. Immunol. 6, 981–988.
Kuo, R.L., Chen, C.J., Wang, R.Y.L., Huang, H.I., Lin, Y.H., Tam, E.H., Tu, W.J., Wu, S.E., Shih, S.R., 2019. Role of enteroviral RNA-dependent RNA polymerase in regulation of MDA5-mediated beta interferon activation. J. Virol. 93.
McCartney, S.A., Thackray, L.B., Gitlin, L., Gilfillan, S., Virgin, H.W., Colonna, M., 2008. MDA-5 recognition of a murine norovirus. PLoS Pathog. 4, e1000108.
McFadden, N., Bailey, D., Carrara, G., Benson, A., Chaudhry, Y., Shortland, A., Heeney, J., Yarovinsky, F., Simmonds, P., Macdonald, A., 2011. Norovirus regulation of the innate immune response and apoptosis occurs via the product of the alternative open reading frame 4. PLoS Pathog. 7, e1002413.
Miller, C.M., Barrett, B.S., Chen, J., Morrison, J.H., Radomile, C., Santiago, M.L., Poeschla, E.M., 2020. Systemic expression of a viral RdRP protects against retrovirus infection and disease. J. Virol. 94, e00071–20.
Moriyama, M., Kato, N., Otsuka, M., Shao, R.X., Taniguchi, H., Kawabe, T., Omata, M., 2007. Interferon-beta is activated by hepatitis C virus NS5B and inhibited by NS4A, NS4B, and NS5A. Hepatol. Int. 1, 302–310.
Nikonov, A., Molder, T., Sikut, R., Kiiver, K., Mannik, A., Toots, U., Lulla, A., Lulla, V., Utt, A., Merits, A., Ustav, M., 2013. RIG-I and MDA-5 detection of viral RNA-dependent RNA polymerase activity restricts positive-strand RNA virus replication. PLoS Pathog. 9, e1003610.
Orchard, R.C., Sullender, M.E., Dunlap, B.F., Balce, D.R., Doench, J.G., Virgin, H.W., 2019. Identification of antinorovirus genes in human cells using genome-wide CRISPR activation screening. J. Virol. 93 e01324-01318.
Orchard, R.C., Wilen, C.B., Doench, J.G., Baldridge, M.T., McCune, B.T., Lee, Y.-C.J., Lee, S., Pruett-Miller, S.M., Nelson, C.A., Fremont, D.H., 2016. Discovery of a proteinaceous cellular receptor for a norovirus. Science 353, 933–936.
Painter, M.M., Morrison, J.H., Zoecklein, L.J., Rinkoski, T.A., Watzlawik, J.O., Papke, L. M., Warrington, A.E., Bieber, A.J., Matchett, W.E., Turkowski, K.L., Poeschla, E.M., Rodriguez, M., 2015. Antiviral protection via RdRP-mediated stable Activation of innate immunity. PLoS Pathog. 11, e1005311.
Schoggins, J.W., Wilson, S.J., Panis, M., Murphy, M.Y., Jones, C.T., Bieniasz, P., Rice, C. M., 2011. A diverse range of gene products are effectors of the type I interferon antiviral response. Nature 472, 481.
Seth, R.B., Sun, L., Ea, C.K., Chen, Z.J., 2005. Identification and characterization of MAVS, a mitochondrial antiviral signaling protein that activates NF-kappaB and IRF 3. Cell 122, 669–682.
Subba-Reddy, C.V., Goodfellow, I., Kao, C.C., 2011. VPg-primed RNA synthesis of norovirus RNA-dependent RNA polymerases by using a novel cell-based assay. J. Virol. 85, 13027–13037.
Wobus, C.E., Karst, S.M., Thackray, L.B., Chang, K.-O., Sosnovtsev, S.V., Belliot, G., Krug, A., Mackenzie, J.M., Green, K.Y., Virgin Iv, H.W., 2004. Replication of Norovirus in cell culture reveals a tropism for dendritic cells and macrophages. PLoS Biol. 2, e432.
Wobus, C.E., Thackray, L.B., Virgin, H.W., 2006. Murine norovirus: a model system to study norovirus biology and pathogenesis. J. Virol. 80, 5104–5112.
Wu, J., Chen, Z.J., 2014. Innate immune sensing and signaling of cytosolic nucleic acids. Annu. Rev. Immunol. 32, 461–488.
Yoneyama, M., Kikuchi, M., Matsumoto, K., Imaizumi, T., Miyagishi, M., Taira, K., Foy, E., Loo, Y.M., Gale Jr., M., Akira, S., Yonehara, S., Kato, A., Fujita, T., 2005. Shared and unique functions of the DExD/H-box helicases RIG-I, MDA5, and LGP2 in antiviral innate immunity. J. Immunol. 175, 2851–2858.
Yoneyama, M., Kikuchi, M., Natsukawa, T., Shinobu, N., Imaizumi, T., Miyagishi, M., Taira, K., Akira, S., Fujita, T., 2004. The RNA helicase RIG-I has an essential function in double-stranded RNA-induced innate antiviral responses. Nat. Immunol. 5, 730–738.

Yu, G.Y., He, G., Li, C.Y., Tang, M., Grivennikov, S., Tsai, W.T., Wu, M.S., Hsu, C.W., Tsai, Y., Wang, L.H., Karin, M., 2012. Hepatic expression of HCV RNA-dependent RNA polymerase triggers innate immune signaling and cytokine production. Mol. Cell. 48, 313–321.

Yu, P., Li, Y., Li, Y., Miao, Z., Peppelenbosch, M.P., Pan, Q., 2020. Guanylate-binding protein 2 orchestrates innate immune responses against murine norovirus and is antagonized by the viral protein NS7. J. Biol. Chem. 295, 8036–8047.

Zamyatkin, D.F., Parra, F., Alonso, J.M.M., Harki, D.A., Peterson, B.R., Grochulski, P., Ng, K.K.S., 2008. Structural insights into mechanisms of catalysis and inhibition in Norwalk virus polymerase. J. Biol. Chem. 283, 7705–7712.

Zhu, S., Regev, D., Watanabe, M., Hickman, D., Moussatche, N., Jesus, D.M., Kahan, S.M., Napthine, S., Brierley, I., Hunter Iii, R.N., 2013. Identification of immune and viral correlates of norovirus protective immunity through comparative study of intra-cluster norovirus strains. PLoS Pathog. 9, e1003592.